

Collaborative Conflict-Free 4D Trajectory Planning Based on Multi-objective Hybrid-Metaheuristic Optimization Algorithm

ZHOU Yi^{1,2}, HU Minghua^{1,2*}, YANG Lei^{1,2}, ZHANG Ying^{2,3}

1. College of Civil Aviation, Nanjing University of Aeronautics and Astronautics, Nanjing 211106, P. R. China;

2. State Key Laboratory of Air Traffic Management System, Nanjing 211106, P. R. China;

3. College of General Aviation and Flight, Nanjing University of Aeronautics and Astronautics, Nanjing 211106, P. R. China

(Received 18 January 2024; revised 20 April 2024; accepted 8 May 2024)

Abstract: To facilitate collaborative decision making in future air traffic management systems under the trajectory based operation framework, a collaborative conflict-free four-dimensional (4D) trajectory planning method is proposed. Firstly, a multi-objective integer linear optimization model is developed to improve flight efficiency and inter-airline equity under conflict-free constraint. Secondly, a Gini coefficient-based metric is formulated to quantify the inter-airline equity of operation cost allocation. Thirdly, to improve the problem-solving efficiency, a grid-based conflict detection method is employed to accelerate conflict detection and a multi-objective hybrid-metaheuristic optimization algorithm (MHMOA) is designed to approximate the optimal non-dominated solutions by combining the simulated annealing (SA) and hill-climbing local search algorithms. Finally, the optimization results of the MHMOA, SA and two conventional multi-objective optimization algorithms are compared and analyzed using the actual flight plan and route network data. The results indicate that MHMOA can obtain higher-quality non-dominated solutions with lower delays, flight level shifts and better equity than other three algorithms, and outperform in terms of three multi-objective optimization performance metrics. The obtained solution can provide more detailed decision support for air traffic managers.

Key words: air traffic management; flight trajectory planning; hybrid-metaheuristic optimization algorithm; four-dimensional (4D) trajectory; multi-objective optimization

CLC number: V355.1

Document code: A

Article ID: 1005-1120(2024)03-0372-15

0 Introduction

With the ever-growing demands of civil aviation transportation, air traffic flow continues to increase, which puts tremendous pressure on current air traffic management systems, and has become a serious problem in the development of the aviation industry. In order to ensure the safe and efficient operation of the future air traffic with increasing demands, the concept of trajectory based operations (TBO) has been proposed. The functionality of air traffic management (ATM) in the TBO framework is to manage flights' trajectories and their interactions to achieve the optimum system outcome with

minimal deviation from the user-requested flight trajectory^[1]. The four-dimensional (4D) trajectories planning is conducive to ensuring flight safety, improving airspace operation efficiency and the economic benefits of flight operations.

According to the time horizon, the flight trajectories planning process can be roughly classified into three phases, which are the strategic-level, the pre-tactical and the tactical phases. The strategic-level trajectory planning involves large-scale flights, which are optimized based on a network-wide view before the day of operations. Its primal intent is for demand and capacity balancing (DCB) and efficiency improvement through network operational plan-

*Corresponding author, E-mail address: minghuahu@nuaa.edu.cn.

How to cite this article: ZHOU Yi, HU Minghua, YANG Lei, et al. Collaborative conflict-free 4D trajectory planning based on multi-objective hybrid-metaheuristic optimization algorithm[J]. Transactions of Nanjing University of Aeronautics and Astronautics, 2024, 41(3): 372-386.

<http://dx.doi.org/10.16356/j.1005-1120.2024.03.009>

ning. Early works on strategic trajectory planning focused on flow optimization with a macroscopic-level description. Bertsimas et al. proposed a mixed 0—1 integer trajectory-based models to minimize flight delays with constraints of airports and sector capacities^[2]. The first model to consider 4D trajectories in air traffic flow management (ATFM) context was proposed by Sherali et al.^[3], which assigns flights to trajectories. Diao et al.^[4] proposed a mathematical formulation of ATFM model with 4D trajectories to minimize total delay, cancellation cost, and fuel burn. Ntakolia et al.^[5] proposed a mixed integer non-linear ATFM model based on 4D trajectories for free flight operation concept to minimize the delay and cancellation costs. However, the macroscopic models failed to consider the detailed traffic situation, and it is challenging to ensure flight operation safety solely through the implementation of DCB measures.

Under TBO context, the 4D trajectory information with greater predictability and precision supported by advanced navigation and communication technology enables the network-wide trajectory deconfliction in strategic phase, which alleviates the workload of air traffic controllers (ATCOs) at tactical intervention. Therefore, instead of focusing on DCB requirements like macroscopic models, recent works have concerned on a microscopic-level traffic situation. These advanced works solve a potential conflict between two aircraft trajectories through different approaches, such as departure time adjustment, rerouting, flight level allocation, or a combination of them. In the STREAM project, sponsored by EUROCONTROL, a new data structure for the grid-based conflict detection method was designed, and a causal model based on flight routing allocation was proposed in view of the “domino effect” of strategic 4D trajectory deconfliction^[6-7]. Wang et al.^[8] combined entry slot allocation and speed control maneuvers to separate trajectories and introduced a physical programming method to address the problem. Juntama^[9] proposed an optimization approach to address the strategic deconfliction problem with the mitigation strategies of departure

time adjustment, rerouting, and flight level allocation, and an extended robust model was designed with the consideration of time uncertainty. Baneshi et al.^[10] proposed a strategic conflict assessment and resolution framework based on the speed control for the climate-optimal trajectories. Zhou et al.^[11] formulated a deconfliction model based on the time geography, which combined the flight level allocation, the rerouting and the speed control to solve conflicts between trajectories. Pérez-Castán et al.^[12] proposed a probabilistic strategic conflict-management method with speed adjustment and rerouting for 4D trajectories in free-route airspace.

With the introduction of accurate 4D trajectories, the trajectories planning problem at the strategic phase may involve thousands of decision variables, which contributes to the application of heuristic algorithms for problem resolution. Liu et al.^[13] combined an ant colony algorithm and the artificial potential field method to improve the efficiency of solving the conflict resolution problem. Courchelle et al.^[14] employed a simulated annealing metaheuristic approach considering the complexity of the strategic aircraft deconfliction problem under wind and temperature uncertainties. Xu et al.^[15] proposed a heuristic approach within the framework of the cooperative co-evolution evolutionary algorithm, which decomposed the problem into sub-problems that evolved separately. Li et al.^[16] combined a genetic algorithm and the adaptive local search operator to propose a memetic algorithm for large-scale strategic conflict resolution. Guo et al.^[17] introduced a knee-guided evolutionary algorithm for large scale 4D trajectories optimization.

A core feature of TBO context is the collaborative decision making (CDM) in sharing and managing trajectories across the ATM system participants. Therefore, the trade-offs exist between different needs and objectives of ATM stakeholders should be considered in trajectories planning. For instance, safety is the primary objective of ATCOs, while the airlines and airport operators concern more about the operation efficiency. Dal et al.^[18] responded to stakeholders’ diverse priorities by developing a tri-

objective optimization method that facilitates CDM through a trade-off between performance metrics. Xu et al.^[19] introduced a collaborative ATFM framework integrating trajectory planning by airlines and ATFM conducted by ATCos. Expanding from this, Zhang et al.^[20] integrated the user-driven prioritization process concept into the collaborative ATFM framework, proposing models to minimize total delay costs. Chen et al.^[21] proposed a visualized trajectory planning method to facilitate CDM between controllers and pilots through trajectory negotiation mechanism.

The problem of strategic-level trajectories planning generally involves the allocation of operation cost or scarce resources among multiple airspace users. Therefore, it is essential to consider equity objective in the strategic-level trajectories planning. The current studies with the explicit use of equity metrics in the ATM field focus on the ATFM initiatives, such as the Ground Delay Program^[22], and airport scheduling^[23]. These equity metrics can be classified into two groups, which are flight-level equity and airline level equity. The flight-level equity metrics consider the fair allocation of cost or resource among individual flights. Most airline-level equity metrics are derived from the equity ratio that measures to what extent the share of airline's cost is proportional to its traffic volume share^[24]. Few researchers incorporate equity consideration in the trajectory conflict resolution. Rey et al.^[25] proposed an equity-oriented approaches for conflict resolution with introduction of flight-level equity metric to fairly distribute the marginal costs among individual flights. However, the inter-airline equity has not been discussed in the studies on strategic conflict-free trajectory planning.

The existing studies on strategic conflict-free trajectory planning mainly focus on minimizing potential conflicts between trajectories, and cannot support the implementation of the CDM philosophy in a TBO environment. In terms of the overall operational efficiency of air traffic, if the safety is the only consideration, unfavorable situations, such as excessive flight costs and maldistribution of flight costs among airlines, may occur, which are incon-

sistent with the concept of CDM with airspace users under the TBO environment. Therefore, the aim of this study is the development of a bi-objective conflict-free flight trajectories planning model able to minimize total trajectory costs and maximize the fairness of cost allocation among different airlines. An equity metric based on the Gini coefficient is employed to assess the inter-airline equity. The grid-based conflict detection method is employed and potential conflicts are resolved through departure time adjustment, rerouting, and flight level allocation. In addition, a multi-objective hybrid-metaheuristic optimization algorithm (MHMOA) is designed to solve this large-scale multi-objective optimization problem. Finally, an empirical study is conducted to evaluate the performance of the proposed algorithm on real data, and solutions achieved by the proposed approach allow air traffic managers to identify the trade-off between total cost and fairness and to facilitate the planning of commonly accepted trajectories by all airspace users.

1 Problem Formulation

In this paper, the airspace structure is modeled as a bounded region $S \subset R^3$. The vertical space of the region is divided into a set of flight levels L and the horizontal space is represented by a directed graph (N, E) , where N is the set of nodes representing all the waypoints and airports involved, and E is the set of arcs that stands for airways. Latitudes and longitudes on the earth surface are converted into (x, y) coordinates through the Gauss-Kruger projection with the center of the projection located at the center of the airspace. For each flight $f \in F$, the subgraph $G^f = (G^f, E^f)$ that represents all the feasible waypoints and arcs that flight may cross is defined. Since only the cruising phase of flight operation is considered, the flight level of starting and ending arc refer to the top of climb and descent, respectively, and the starting arc for subgraph G^f is denoted as $orig_f \in E^f$. Meanwhile, flights are assumed to fly at constant cruising speeds along the planed trajectories. The notation for model formulation is listed in Table 1.

Table 1 Notations and definitions

Notation	Definition
F	Set of flights, $f \in F$
A	Set of airlines, $a \in A$
$G^f = (N^f, E^f)$	Feasible network for flight f
L^f	Set of feasible flight levels for flight f , $l' \in L^f$
T	Set of time-slots, $t \in T$
F_a	Set of flights belonging to airline a
O_e^f	Set of arcs leaving the head node of arc $e \in E^f$
I_e^f	Set of arcs entering the tail node of arc $e \in E^f$
$T_e^f = \left[\begin{matrix} T_e^f \\ \bar{T}_e^f \end{matrix} \right]$	Set of feasible time periods to fly arc e for flight f
α_e^f	Flight time to travel arc e by flight f
t_{sche}^f	Scheduled departure time for flight f
l_{sche}^f	Scheduled flight level for flight f
$C_{e,l}^f$	Cost of traveling arc e at level l for flight f
r^f	Number of alternative routes for flight f
Φ_f	Number of conflicts for flight f
K^f	Number of sampled points for flight f
δ^f	Maximum allowed ground delay for flight f
ρ^f	Maximum allowed flight level shift for flight f
λ^{GH}	Coefficient for ground delay cost
λ^{RT}	Coefficient for route flight cost
λ^{FL}	Coefficient for flight level allocation cost

1.1 Decision variables and objectives

The following binary variables are introduced as the decision variables for the model

$$x_{e,l}^f(t) = \begin{cases} 1 & \text{Flight } f \text{ traverses arc } e \text{ at flight level } l \text{ by time } t \\ 0 & \text{Otherwise} \end{cases}$$

To avoid potential conflicts, the flight may deviate from its planned trajectory, which results in the extra flight operation cost. Thus, the first objective considered in the model is to minimize the total trajectory modification cost (TTMC), which consists of ground delay cost (Cost_{GH}), route flight cost (Cost_{RT}) and flight level allocation cost (Cost_{FL}). It can be expressed as a weighted sum of these three normalized costs

$$\min \text{TTMC} = (\lambda^{\text{GH}} \text{Cost}_{\text{GH}} + \lambda^{\text{RT}} \text{Cost}_{\text{RT}} + \lambda^{\text{FL}} \text{Cost}_{\text{FL}}) \quad (1)$$

where λ^{GH} , λ^{RT} , λ^{FL} are the cost coefficients for the three parts, which reflect the relative importance of each cost from the airline perspective.

(1) Ground delay cost

In the strategic planning phase, airborne holding and speed adjustment are not the commonly used maneuver options for the conflict resolution process. Therefore, only the ground delay cost derived from the departure time adjustment is considered.

$$\text{Cost}_{\text{GH}} = \sum_{f \in F, l \in T, l' \in L^f} (t - t_{\text{sche}}^f) (x_{\text{orig},l}^f(t) - x_{\text{orig},l}^f(t-1)) \quad (2)$$

(2) Route flight cost

To improve the flight operation efficiency and participation of airspace users in collaborative decision-making process of air traffic management, airlines can provide air traffic managers with the sets of alternative planned routes and corresponding route costs $C_{e,l}^f$ for their flights.

$$\text{Cost}_{\text{RT}} = \sum_{f \in F, e \in E^f, l \in L^f} C_{e,l}^f x_{e,l}^f(\bar{T}_e^f) \quad (3)$$

(3) Flight level allocation cost

Deviating from the most economical flight level, namely the scheduled flight level, causes the extra flight operation costs. The flight level allocation cost is related to the number of the flight levels that a flight deviates from its scheduled flight level.

$$\text{Cost}_{\text{FL}} = \sum_{f \in F, l \in T, l' \in L^f} |l' - l_{\text{sche}}^f| (x_{\text{orig},l'}^f(t) - x_{\text{orig},l'}^f(t-1)) \quad (4)$$

If the conflict resolution process only concentrates on the flight cost reduction, the proposed trajectory plan may force some airlines to pay higher trajectory modification cost in order to avoid conflicts and reduce TTMC, which results in the maldistribution of airline's total trajectory modification cost (ATTMC), and undermines the fairness of the aviation market. As a generally accepted metric of fairness, Gini coefficient has been adopted in the field of air traffic management to assess the inequality of resource allocation between different stakeholders^[26-28]. Therefore, the Gini coefficient is intro-

duced to measure the overall fairness in ATTMC allocation of the proposed trajectory plan. The original way to define Gini coefficient is based on the relative mean difference. Specifically, given n income observations (x_1, x_2, \dots, x_n) , the Gini coefficient, denoted as GINI, can be calculated as

$$\text{GINI} = \frac{\sum_{i=1}^n \sum_{j=1}^n |x_i - x_j|}{2n \sum_{i=1}^n x_i} \quad (5)$$

After sorting the n income observations in a non-decreasing order $(x_1^* \leq x_2^* \leq \dots \leq x_n^*)$, the Gini coefficient can be rewritten as

$$\text{GINI} = \frac{n+1}{n} - \frac{2 \sum_{i=1}^n (n+1-i)x_i^*}{n \sum_{i=1}^n x_i} \quad (6)$$

Now we adapt the above GINI to the 4D trajectory planning context. We replace x_i by the ATTMC of each airline, and sort the airlines by their ATTMC in a non-decreasing order. The ATTMC of the airline a in the sorted airline set A^* is denoted as ATTMC_a^* . The number of airlines in set A is denoted as $|A|$. The inter-airline equity is calculated as

$$\text{GINI} = \frac{|A|+1}{|A|} - \frac{2 \sum_{a \in A^*} (|A|+1-a) \text{ATTMC}_a^*}{|A| \sum_{a \in A} \text{ATTMC}_a} \quad (7)$$

$$\text{ATTMC}_a = \sum_{f \in F_a} \text{TTMC}_f \quad (8)$$

1.2 Constraints

1.2.1 Conflict-free constraint

When the distance between two aircraft violates the minimum separation requirement enforced by the International Civil Aviation Organization (5 NM horizontally and 1 000 ft vertically), the aircraft involved are considered to be in conflict. Due to excessive computation time requirements of the traditional pairwise conflict detection method, the grid-based conflict detection method^[29-30] is employed in this paper to improve the efficiency of conflict detection. The main process of this method is described as follows.

The airspace is firstly discretized through a 4D space-time grid. Then, trajectory sampled points

$P_{f,k}$ of each flight f are mapped to the corresponding grid cells according to their 4D coordinates. This detection method only needs to check $3^3 = 27$ neighboring cells around the corresponding cell of the sampled point $P_{f,k}$, which serves as the preliminary selection process to avoid unnecessary pairwise comparisons. As depicted in Fig.1, if there are trajectory sampled points of other flights in the surrounding cells, the horizontal distance and vertical distance between this pair of sampled points are calculated for judgment. If the minimum separation requirement is violated, the flight f has a conflict at the k th trajectory sampled point $P_{f,k}$ ($\Phi_{f,k} = 1$). The total number of conflicts for one flight is calculated by summing up the conflict number of all sampled points along its flight trajectory.

$$\Phi_f = \sum_{k=1}^{K'} \Phi_{f,k} \quad (9)$$

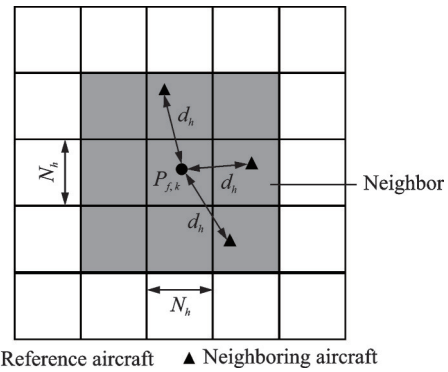


Fig.1 Grid-based conflict detection in horizontal plane

The sum of conflicts associated with every flight in the airspace can be used for conflict constraint representation.

$$\Phi_{\text{total}} = \sum_{f \in F} \Phi_f \quad (10)$$

When the total number of conflicts is zero, the generated trajectories are ensured to be conflict-free.

$$\Phi_{\text{total}} = 0 \quad \forall f \in F \quad (11)$$

1.2.2 Other constraints

Constraints (12–14) ensure that each flight follows one single feasible trajectory. Constraint (15) imposes that the departure time of one flight does not exceed its pre-defined upper limit. Constraint (16) means that the maximum number of al-

ternative routes for one flight is n . Constraint (17) indicates that the flight level shift for one flight needs to be within certain range. Constraint (18) describes the upper boundary l_{\max}^f and lower boundary l_{\min}^f of feasible flight level for each flight, which is determined by the operational regulation and performance envelope of specific aircraft type provided by base of aircraft data (BADA).

$$\begin{cases} x_{e,l}^f(t) \leq \sum_{e' \in O_e^f, l' \in L^f} x_{e',l'}^f(t + \alpha_e^f) \\ \forall f \in F, e \in E^f, l \in L^f, t \in T_e^f \end{cases} \quad (12)$$

$$\begin{cases} \sum_{l \in L^f} x_{e,l}^f(\bar{T}_e^f) \leq \sum_{e' \in I_e^f, l' \in L^f} x_{e',l'}^f(\bar{T}_e^f) \\ \forall f \in F, e \in E^f \end{cases} \quad (13)$$

$$\begin{cases} x_{e,l}^f(t-1) - x_{e,l}^f(t) \leq 0 \\ \forall f \in F, e \in E^f, l \in L^f, t \in T_e^f \end{cases} \quad (14)$$

$$\begin{cases} (t - t_{\text{sche}}^f)(x_{\text{orig},l}^f(t) - x_{\text{orig},l}^f(t-1)) \leq \delta^f \\ \forall f \in F, l \in L^f, t \in T_e^f \end{cases} \quad (15)$$

$$1 \leq r^f \leq n \quad \forall f \in F \quad (16)$$

$$\begin{cases} |l^f - l_{\text{sche}}^f| (x_{\text{orig},l}^f(t) - x_{\text{orig},l}^f(t-1)) \leq \rho^f \\ \forall f \in F, l \in L^f, t \in T_e^f \end{cases} \quad (17)$$

$$\begin{cases} l_{\min}^f \leq l^f (x_{\text{orig},l}^f(t) - x_{\text{orig},l}^f(t-1)) \leq l_{\max}^f \\ \forall f \in F, l \in L^f, t \in T_e^f \end{cases} \quad (18)$$

2 Resolution Algorithm

To solve the large-scale multi-objective optimization problem mentioned above, a multi-objective hybrid-metaheuristic optimization algorithm (MHMOA) is presented to approximate the Pareto optimal frontier. The proposed MHMOA combines simulated annealing algorithm (SA) and the hill-climbing local search such that the local search is considered as an inner-loop of the SA, which will be performed when a pre-defined condition is satisfied. The local search algorithm is used to intensify the search of the solution space around a potential feasible solution, while SA can avoid the algorithm being trapped into the local optimum by accepting degraded solutions with probability. An external archive is introduced to store the non-dominated solutions. The structure of the proposed hybrid multi-objective algorithm of SA and hill-climbing local search methods is depicted in Fig.2.

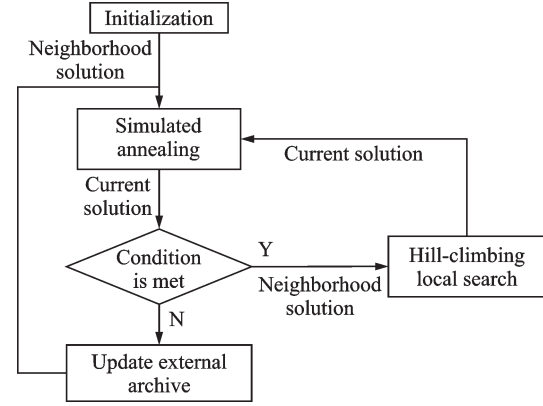


Fig.2 Structure of the proposed MHMOA

2.1 Algorithm execution probability

The condition of algorithm execution is controlled by pre-defined parameters that control the probabilities to conduct each algorithm.

(1) The probability of carrying out SA is defined as

$$P_{\text{SA}}(\Gamma) = P_{\text{SA}, \min} + (P_{\text{SA}, \max} - P_{\text{SA}, \min}) \cdot \frac{\Gamma_0 - \Gamma}{\Gamma_0} \quad (19)$$

where $P_{\text{SA}, \min}$ and $P_{\text{SA}, \max}$ are the minimum and maximum probabilities of running SA; and Γ_0 and Γ the initial temperature and the current temperature, respectively.

(2) The probability of performing the local search algorithm is defined as

$$P_{\text{LOC}}(\Gamma) = P_{\text{LOC}, \min} + (P_{\text{LOC}, \max} - P_{\text{LOC}, \min}) \cdot \frac{\Gamma_0 - \Gamma}{\Gamma_0} \quad (20)$$

where $P_{\text{LOC}, \min}$ and $P_{\text{LOC}, \max}$ are the minimum and the maximum probabilities to carry out the local search algorithm, respectively.

(3) The probability of running both SA and the local search algorithm in sequence is

$$P_{\text{SL}}(\Gamma) = 1 - (P_{\text{SA}}(\Gamma) + P_{\text{LOC}}(\Gamma)) \quad (21)$$

2.2 Neighborhood structure and external archive

The definition of the neighborhood structure is a key part of MHMOA, which contributes to the neighborhood solution generation of both SA and hill-climbing local search. A neighborhood solution is generated by applying a local change from the neighborhood structure to trajectory i selected from current solution. To increase the number of feasible solutions that satisfy the conflict constraint, the rou-

lette selection method is adopted to select the trajectory for the local change.

According to the conflict detection result, if the conflict exists, the probability for each trajectory to be selected is determined in proportion to its conflict number Φ_i . Then, the cumulative probability is calculated based on the trajectory selection probability. A value in $[0, 1]$ is generated randomly, and the trajectory i is selected according to the cumulative probability interval in which this random value lies. If there is no conflict, the trajectory for local change is randomly selected. For the selected trajectory i , three maneuver options could be used for conflict resolution, including ground delays, rerouting and flight level allocations. To allow airspace users to express their preference on the maneuver options of conflict resolution, two user-defined parameters, P_{GH} and P_{FL} , between $[0, 1]$ are introduced, which control the probability of performing ground delay and the flight level allocation on the trajectory i , respectively. Therefore, the probability of rerouting trajectory i is $1 - P_{GH} - P_{FL}$. The process of neighborhood structure in this paper is presented in Fig. 3.

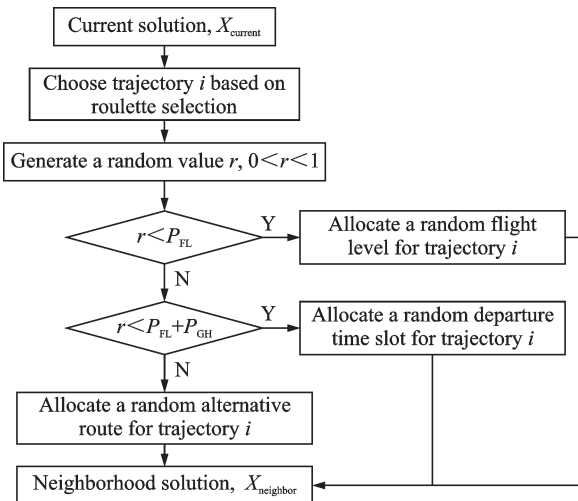


Fig. 3 Flow chart of neighborhood structure

After evaluating the generated neighborhood solution, the algorithm needs to determine whether it improves objectives compared with the current solution and whether to accept it as the new current solution. Hence, it is necessary to specify the acceptance criterion. If the neighborhood solution violates the conflict constraint, the solution with the reduced

number of conflicts will be accepted. Conversely, if the conflict constraint is satisfied, TTMC and the Gini coefficient of the neighborhood solution are evaluated, and the algorithm accepts the solution that reduces the value of either objective. Then, the updated solution is adopted to determine nondominated solutions.

An external archive E is introduced to save the current nondominated solutions during the optimization process. In the initialization phase, the external archive E is an empty set. Whenever a new solution $X_{current}$ is generated, we firstly determine whether $X_{current}$ dominates any solution of the current external population E . If this situation exists, the solutions dominated by $X_{current}$ will be removed out of E , and $X_{current}$ will be added to E . If there is no solution in E dominated by $X_{current}$, then we determine whether there are solutions in E dominate $X_{current}$. If there is no individual dominating $X_{current}$, $X_{current}$ and all individuals in E are mutually nondominated. $X_{current}$ will then become a new non-dominated solution and will be added to E . At the end of the algorithm, E is just the Pareto-optimal set. The detailed steps of updating the external archive are shown in Algorithm 1.

Algorithm 1 The external archive update

Input: A current solution $X_{current}$;

Output: An external archive E .

- (1) If $(|E| = 0)$ then
- (2) Add $X_{current}$ to E ;
- (3) Else if $(X_{current}$ dominates any archive member) then
- (4) Delete dominated members in E ;
- (5) Add $X_{current}$ to E ;
- (6) Else if $(X_{current}$ is dominated by any archive member) then
- (7) Exit;
- (8) Else
- (9) Add $X_{current}$ to E ;
- (10) End if
- (11) End

2.3 Simulated annealing and local search algorithm

The simulated annealing algorithm is a stochas-

tic searching optimization algorithm based on the Monte Carlo iterative method, and the Metropolis algorithm is used to simulate this evolution of the physical system toward a thermal equilibrium^[31]. For the temperature T of each iteration, the decision variables are modified based on the neighborhood structure mentioned above to generate a neighborhood solution. If the generated neighborhood solution satisfies the pre-defined acceptance criterion, this solution is accepted. Otherwise, the degraded solution is accepted with probability

$$p = e^{-\frac{\Delta E}{T}} \quad (22)$$

where ΔE refers to the degradation of the fitness function value. In order to calculate ΔE , the weighted sum method is used in this paper to combine the values of two objectives, and the number of conflicts is added as a penalty term. ΔE is the difference in the results of weighted sum method between the current solution and the new solution, which is defined as

$$\Delta E = \text{fit}(X_{\text{current}}) - \text{fit}(X_{\text{neighbor}}) \quad (23)$$

$$\text{fit} = M \cdot \Phi_{\text{total}} + \text{TTMC}' + \text{GINI}' \quad (24)$$

where $\text{fit}(X_{\text{current}})$, $\text{fit}(X_{\text{neighbor}})$ are the values of fitness function for current and newly generated solutions, respectively; TTMC' and GINI' are the normalized values of TTMC and Gini coefficients, respectively; M is the conflict penalty weight coefficient, which is set as 2 to ensure that weighted conflict number exceeds the sum of normalized values of the two considered objectives.

If the maximum number of iterations N_1 at a given temperature is reached, the temperature is decreased with $T_{i+1} = \alpha \cdot T_i$, and this process is repeated until the pre-defined final temperature T_f is reached. At each iteration of the hill-climbing local search algorithm, the solution space around the current solution is searched for a local optimal solution to update the current solution. First, a neighborhood solution is generated by applying local change to the current solution according to the above-mentioned neighborhood structure. Then, the algorithm only accepts the neighborhood solution, which meets the acceptance criteria, as the new current so-

lution. This process is repeated until reaching the maximum number of iterations n_1 . The MHMOA is detailed in Fig.4.

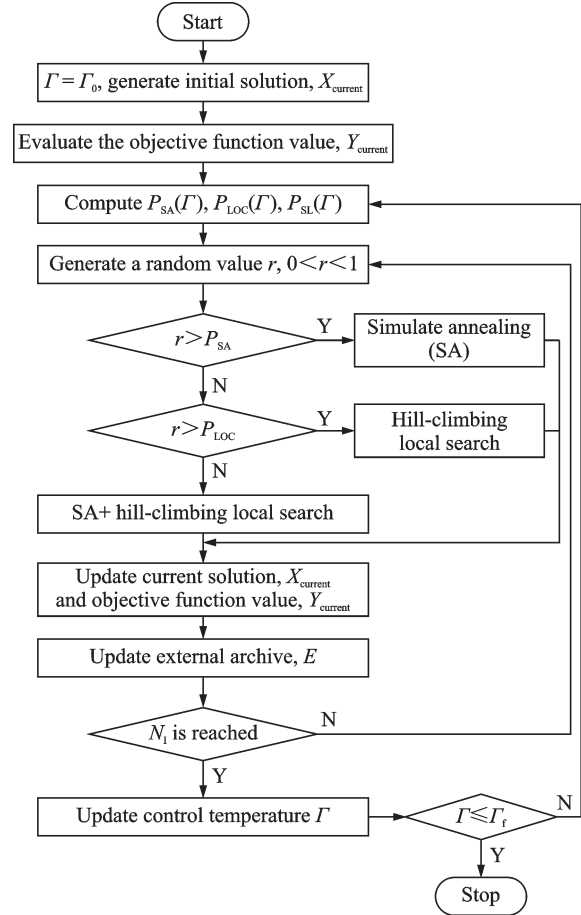


Fig.4 Flow chart of MHMOA

3 Numerical Results

In this paper, real domestic historical flight plan data and flight route network data of China were used to test the performance of the proposed model and algorithm. The selected flight plan was between 8:00 am and 9:00 am on July 3, 2019, involving 2 122 waypoints, 58 airports, and 100 flights. The examples of the flight plan and airway point data are listed in the appendix (Tables A1, A2). It should be noted that the speed of each flight is set based on the corresponding reference vertical profile for its aircraft type provided by BADA. The initial flight trajectories were generated based on the initial flight plan. Besides the flight planned route, the Dijkstra's algorithm was employed to generate the first three shortest rerouting paths between each

city pair as alternative routes. Since airlines are reluctant to share the information about the cost of alternative routes, the route flight cost of each alternative route for each city pair is expressed by its extra airborne flight time relative to the shortest route, namely the airborne delay time. The algorithms were all implemented in MATLAB R2016a, installed on a Windows Server with 2.10 GHz CPU and 16 GB RAM, and all experimental results were collected and analyzed based on 20 independent runs.

3.1 Parameter sensitivity analysis

The parameter settings of the optimization model and MHMOA are listed in Tables 2, 3, respectively. According to the estimation by Cook and Tanner^[32], the ground delay should be less costly than airborne delay and the cost of one-minute airborne delay is two to three times higher than the cost of one-minute delay on the ground. The relationship between flight level shift costs and time-related costs is rarely studied and is beyond the scope of this paper. For simplification, the flight level allocation costs are assumed to be equally important as ground delay costs in this paper, and thus the weight coefficients for three normalized costs are set to 1:3:1 as shown in Table 2.

As a preliminary step for the calculation of the initial temperature Γ_0 , the average value of ΔE is calculated based on 100 random disturbances of the initial solution. Then, Γ_0 could be derived from: $e^{\Delta E/\Gamma_0} = \tau_0$, where τ_0 is the initial rate of acceptance of degraded solutions. Some of the MHMOA pa-

Table 2 Parameters related to the optimization model

Parameter	Value
Length of grid cell/NM	5
Height of grid cell/ft	1 000
Discretization time step $\Delta t/s$	20
λ^{GH}	1
λ^{RT}	3
λ^{FL}	1
δ^f/min	60
Discretization step of departure time/min	5
Maximum number of alternative routes n	4
ρ^f	3

Table 3 Parameters related to MHMOA

Parameter	Value
N_1	100
n_1	5
τ_0	0.4
Temperature reduction coefficient α	0.99
Γ_f	$\Gamma_0/1\ 000$
P_{FL}	0.7
P_{GH}	0.1
$P_{\text{SA}, \text{min}}$	0.8
$P_{\text{SA}, \text{max}}$	0.9
$P_{\text{LOC}, \text{min}}$	0.4
$P_{\text{LOC}, \text{max}}$	0.6

rameters were well-tuned based on the sensitivity analysis results shown in Fig.5. In this paper, the hypervolume (HV) metric is introduced to assess the quality of the non-dominated solution obtained by MHMOA. The parameter values with the highest average HV value were selected and recorded in Table 3.

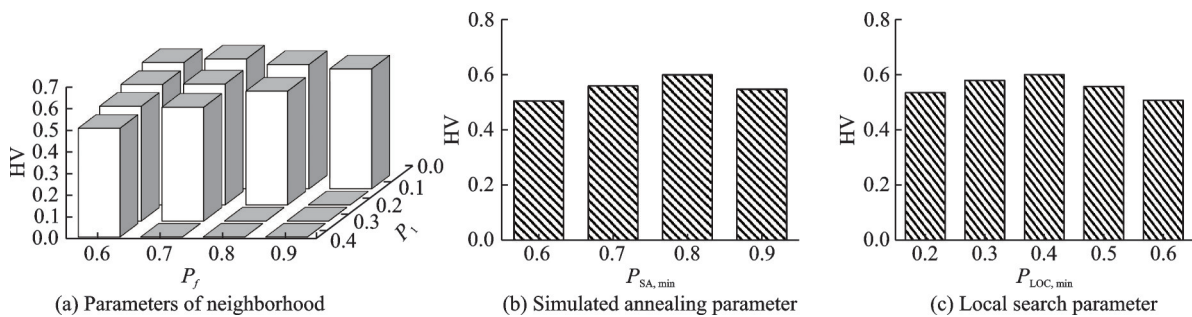


Fig.5 Sensitivity analysis of different parameters for MHMOA

3.2 MHMOA effectiveness

In order to assess the efficiency of MHMOA,

multiple comparison analyses between MHMOA and other algorithms were conducted. Firstly, to

verify the advantages in conflict resolution of combination of SA with local search and roulette selection strategy adopted in MHMOA, another three algorithms with same parameter setting and different strategies were conducted for comparison. Fig.6 depicts the change in the average value of total conflict number with the number of iterations. Comparing the corresponding decline curve of MHMOA and SA, it is shown that the MHMOA can reduce the number of conflicts faster than SA, indicating that adding a local search algorithm can effectively improve the effectiveness of deconfliction between trajectories. In addition, two different strategies of trajectory selection in the neighborhood structure were tested, including roulette selection and random selection. The curves of different trajectory-selection strategies in Fig.6 show that the roulette selection method based on the number of conflicts can significantly increase the efficiency of conflict resolution.

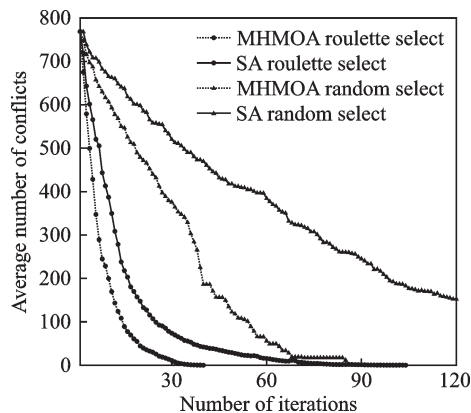


Fig.6 Curves of average number of conflicts versus number of iterations resulted from different algorithms

To verify the efficiency of proposed MHMOA in multi-objective optimization, comparison tests were conducted with SA and two commonly used multi-objective algorithms, including nondominated sorting genetic algorithm (NSGA-II) and multi-objective evolutionary algorithm based on decomposition (MOEA/D). Fig.7 shows the non-dominated solutions of four compared algorithms over 20 independent runs. It can be seen that the non-dominated solutions obtained by MHMOA totally dominate those obtained by other three algorithms, in terms of both total trajectory modification cost and Gini co-

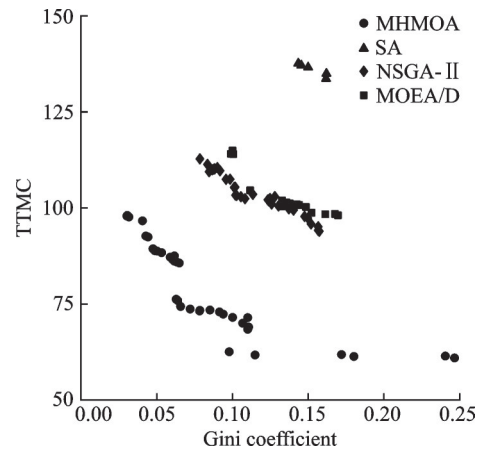


Fig.7 Non-dominated solutions of four compared algorithms

efficient. This indicates that MHMOA outperforms other three algorithms with respect to computational efficiency.

To quantitatively evaluate the set of the non-dominated solutions calculated by the four algorithms, three favorable metrics, namely HV, the generational distance (GD) and the spread (Δ) were introduced to assess the convergency, diversity and overall performance, respectively. The GD indicator measures how far the non-dominated solutions are away from the Pareto optimal frontier. The smaller this indicator is, the better the approximation of the Pareto frontier the algorithm gets. The spread indicator measures the extent of spread by the set of non-dominated solutions. This indicator takes a zero value for an ideal distribution, pointing out a perfect spread of the solutions in the Pareto frontier. The HV is a comprehensive indicator, which calculates the volume in the objective domain covered by the set of non-dominated solutions. For the minimum optimization, a higher HV value means the non-dominated solutions has a better convergence and diversity. The average values and standard deviations (in brackets) of HV, GD, and Δ for the four algorithms are listed in Table 4. Compared with the other three algorithms, the non-dominated solutions obtained by MHMOA have the lowest average values of GD and Δ , and highest average values of HV, which indicates that the MHMOA can generate non-dominated solutions with better convergency, diversity and overall perfor-

mance for the large-scale multi-objective model mentioned in this paper than the other three algorithms.

Table 4 Comparison of the solving efficiency of four algorithms based on three different metrics

Method	HV	GD	Δ
MHMOA	0.592 (0.006)	0.067 (0.038)	0.850 (0.110)
SA	0.501 (0.012)	0.122 (0.071)	0.883 (0.133)
NSGA-II	0.563 (0.009)	0.087 (0.020)	0.861 (0.105)
MOEA/D	0.557 (0.011)	0.091 (0.033)	0.867 (0.097)

3.3 Analysis of optimization results

Fig.8 exhibits the distribution of the ground delay, airborne delay and flight level shift of the solutions obtained by the four compared algorithms. With regard to the ground delay distribution, based on the four algorithms, most flights departed on time without any ground delay. Compared to the other three algorithms, the solutions of MHMOA provide a higher proportion of flights without ground delay and a lower proportion of flights in each delay time interval. For the four compared algorithms, the airborne delay time of most flights lied within

the interval of (0, 5) min. In addition, the proportion of flights without airborne delay derived from MHMOA is slightly higher than those derived from the other three algorithms. The distribution of the flight level shift exhibits similar characteristics with the ground delay distribution. The flights with no flight level shift account for the largest proportion for the both algorithms. In the solutions obtained by MHMOA, the proportion of flights without flight level shift is higher than that obtained by the other three algorithms, while in each range of flight level shift, the proportion of flights is relatively lower.

In Table 5, the average ground delay time (avr_{GH}), average airborne delay time (avr_{AD}), average flight level shift (avr_{FL}) and standard deviation of ATTMC allocation among airlines ($std_{Airlines}$) derived from the four compared algorithms are presented. The comparison of the average values of the first three metrics reveals that MHMOA has superior optimization performance than the other three algorithms with respect to flight cost reduction. According to the standard deviation of ATTMC allocation, the MHMOA solutions have smaller difference in ATTMC allocation among different airlines compared to the other three algorithms, which indicates that MHMOA outperforms the other three algorithms in terms of fairness metric optimization.

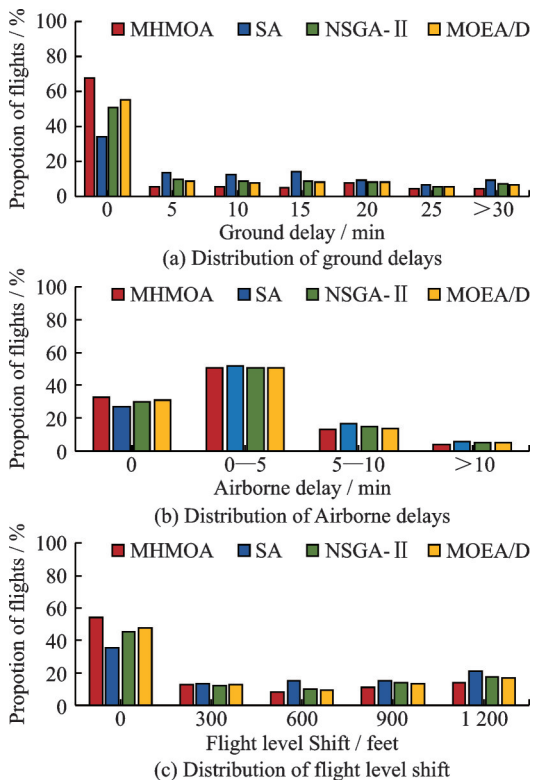


Fig.8 Distribution of ground delays, airborne delays and flight level shift based on four compared algorithms

Table 5 Comparison of the optimization results of four algorithms

Method	avr_{GH}/s	avr_{AD}/s	avr_{FL}/ft	$std_{Airlines}$
MHMOA	466.85	152.65	516.92	2.04
SA	675.19	189.24	546.78	5.92
NSGA-II	571.54	168.33	527.36	3.11
MOEA/D	557.65	165.15	525.14	3.23

To validate the advantages of using Gini coefficient in inter-airline fairness measurement, other two approaches were conducted for comparison, with inter-airline metric based on the maximum deviation of equity ratio (MDER)^[23] and the inter-flight metric based on the Gini coefficient. Fig.9 exhibits the ATTMC distribution of the optimal fairness solutions obtained through three approaches with different fairness metrics. It can be seen that both ap-

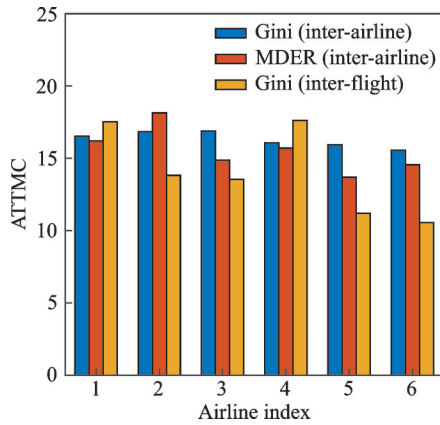


Fig.9 Distribution of ATTMC for solutions obtained by three approached with different fairness metrics

proaches based on the inter-airline metrics can obtain solutions with more evenly distributed ATTMC among airlines compared with the method based on inter-flight metric. In addition, the ATTMC distribution of the proposed approach with Gini coefficient is more evenly than the MDER-based approach.

To analyze the optimization results from the individual level, the flight with the maximum number of conflicts in the initial flight plan was selected as an example. The selected flight had 84 conflicts with seven flights belonging to other airlines in the initial plan, all of which were resolved in the optimized solutions. Table 6 exhibits the ground delay (GD), airborne delay (AD), flight level shift (FLS) and ratio of cost (ROC) of the selected flight in the solutions with minimum TTMC and minimum Gini coefficient respectively. The ROC refers to the ratio of the trajectory modification cost of the selected flight to the total cost of all eight conflicting flights. Compared with the solution with minimum Gini coefficient, the selected flight in the solution with minimum TTMC has lower deviations

Table 6 Comparison of deviation and fairness metrics for selected flight in optimal cost and optimal fairness solutions

Indicator	Min. TTMC	Min. Gini
GD/s	1 200	1 500
AD/s	252	306
FLS/ft	300	600
ROC/%	64	37

from initial planned trajectory in terms of GD, AD and FLS, while it bears a larger ROC in the group of conflicting flights, leading to a degradation of fairness in cost distribution among airlines.

4 Conclusions

An efficient methodology to address flight trajectories planning at the strategic phase is introduced, based on the concept of TBO. Compared with the previous work, a multi-objective optimization model for the conflict-free flight trajectories planning is developed, which relies on approaches including departure time adjustment, rerouting and flight level allocation to modify the initial flight plan for conflict resolution. To take more factors into consideration in the flight trajectory planning process, the minimization of the total trajectory modification cost and the maximization of fairness are set as objectives of the model. In addition, the Gini coefficient is introduced as an indicator to measure the fairness of the trajectory modification cost distribution among airlines. To improve the efficiency of the optimization, a grid-based conflict detection method is employed to accelerate the conflict detection process between trajectories, and a hybrid-metaheuristic optimization algorithm, which combines the simulated annealing and hill-climbing local search algorithm, is developed to solve the model. The proposed methodology is tested with real flight plan and route network data of China. The results demonstrate that the proposed hybrid-metaheuristic optimization algorithm is superior to SA, NSGA-II and MOEA/D in both the effectiveness and optimization performance, which suggests that it can effectively deal with the problem of conflict-free flight trajectories planning.

In the future research, we will further investigate the impact of the aircraft performance on trajectory planning. More precise trajectory adjustment methods will be adopted, such as speed regulation. In addition, the fuel-related costs will be introduced to quantify the impact of the deviation from user-preferred trajectories.

Appendix:

Table A1 Examples of flight plan data used in the test case

Callsign	Aircraft type	Departure AD	Arrival AD	ETD	Scheduled FL/ft
CCA1835	A333	ZBAA	ZSPD	8:05:00	33 100
CSH9345	B738	ZSPD	ZHCC	8:05:00	34 100
DKH1360	A320	ZSPD	ZYTX	8:10:00	35 100
CSZ9539	B738	ZSWX	ZBYN	8:10:00	32 100
CES2035	B738	ZBAA	ZPPP	8:15:00	36 100
CSN3578	A321	ZSNJ	ZGSZ	8:15:00	34 100
CES2152	A321	ZSSS	ZLXY	8:20:00	35 100
CHH7604	B738	ZSSS	ZBAA	8:25:00	34 100

Table A2 Examples of airway point data used in the test case

Airway point name	Code	Latitude/(°)	Longitude/(°)
DAWANGZHUANG	VYK	39.193 28	116.573 52
PUDONG	PD	31.170 61	121.782 41
BUTPO	BUTPO	41.835 83	112.904 17
IRVAG	IRVAG	40.535 28	111.850 56
TEDIB	TEDIB	38.432 22	113.839 44
LADIX	LADIX	39.129 44	116.992 22

References

- [1] GARDI A, SABATINI R, KISTAN T. Multi-objective 4D trajectory optimization for integrated avionics and air traffic management systems[J]. IEEE Transactions on Aerospace and Electronic Systems, 2018, 55(1): 170-181.
- [2] BERTSIMAS D, LULLI G, ODONI A. An integer optimization approach to large-scale air traffic flow management[J]. Operations Research, 2011, 59(1): 211-227.
- [3] SHERALI H D, COLE SMITH J, TRANI A A. An airspace planning model for selecting flight-plans under workload, safety, and equity considerations[J]. Transportation Science, 2002, 36(4): 378-397.
- [4] DIAO X, CHEN C H. A sequence model for air traffic flow management rerouting problem[J]. Transportation Research Part E: Logistics and Transportation Review, 2018, 110: 15-30.
- [5] NTAKOLIA C, LYRIDIS D V. A n-D ant colony optimization with fuzzy logic for air traffic flow management[J]. Operational Research, 2022, 22(5): 5035-5053.
- [6] RUIZ S. Strategic trajectory de-confliction to enable seamless aircraft conflict management[D]. Barcelona, Spain: Universitat Autònoma de Barcelona, 2014.
- [7] RUIZ S, PIERA M A, NOSEDAL J, et al. Strategic de-confliction in the presence of a large number of 4D trajectories using a causal modeling approach[J]. Transportation Research Part C: Emerging Technologies, 2014, 39: 129-147.
- [8] WANG H, DONG Z, DENG T, et al. En route sector complexity control strategies in air traffic management[J]. Transaction of Nanjing University of Aeronautics and Astronautics, 2021, 38(6): 901-913.
- [9] JUNTAMA P. Large scale adaptive 4D trajectory planning[D]. Toulouse, France: Université Paul Sabatier-Toulouse III, 2022.
- [10] BANESHI F, SOLER M, SIMORGH A. Conflict assessment and resolution of climate-optimal aircraft trajectories at network scale[J]. Transportation Research Part D: Transport and Environment, 2023, 115: 103592.
- [11] ZHOU Y, HU M, YANG L, et al. Autonomous and collaborative trajectory planning for traffic complexity management[J]. IET Intelligent Transport Systems, 2023, 17(5): 992-1008.
- [12] PÉREZ-CASTÁN J A, RODRÍGUEZ-SANZ Á, PÉREZ SANZ L, et al. Probabilistic strategic conflict-management for 4D trajectories in free-route airspace[J]. Entropy, 2020, 22(2): 159.
- [13] LIU H X, LIU F, ZHANG X J, et al. Aircraft conflict resolution method based on hybrid ant colony optimization and artificial potential field[J]. Science China Information Sciences, 2018, 61(12): 129103.

- [14] COURCHELLE V, SOLER M, GONZÁLEZ-ARRIBAS D, et al. A simulated annealing approach to 3D strategic aircraft deconfliction based on en-route speed changes under wind and temperature uncertainties[J]. *Transportation Research Part C: Emerging Technologies*, 2019, 103: 194-210.
- [15] XU M, HU M, ZHOU Y, et al. Multi-aircraft cooperative strategic trajectory-planning method considering wind forecast uncertainty[J]. *Sustainability*, 2022, 14(17): 10811.
- [16] LI B, GUO T, MEI Y, et al. A multi-objective memetic algorithm with adaptive local search for airspace complexity mitigation[J]. *Swarm and Evolutionary Computation*, 2023, 83: 101400.
- [17] GUO T, MEI Y, TANG K, et al. A knee-guided evolutionary algorithm for multi-objective air traffic flow management[J/OL]. *IEEE Transactions on Evolutionary Computation*, 2023. <https://ieeexplore.ieee.org/document/10142158>.
- [18] DAL S V, FOMENI F D, LULLI G, et al. Planning efficient 4D trajectories in air traffic flow management[J]. *European Journal of Operational Research*, 2019, 276(2): 676-687.
- [19] XU Y, DALMAU R, MELGOSA M, et al. A framework for collaborative air traffic flow management minimizing costs for airspace users: Enabling trajectory options and flexible pre-tactical delay management[J]. *Transportation Research Part B: Methodological*, 2020, 134: 229-255.
- [20] ZHANG Q, LE M, XU Y. Collaborative delay management towards demand-capacity balancing within user driven prioritisation process[J]. *Journal of Air Transport Management*, 2021, 91: 102017.
- [21] CHEN Y, HU M, YANG L. Autonomous planning of optimal four-dimensional trajectory for real-time en-route airspace operation with solution space visualisation[J]. *Transportation Research Part C: Emerging Technologies*, 2022, 140: 103701.
- [22] JIANG Y, ZOGRAFOS K G. A decision making framework for incorporating fairness in allocating slots at capacity-constrained airports[J]. *Transportation Research Part C: Emerging Technologies*, 2021, 126: 103039.
- [23] GUO Y, HU M, ZOU B, et al. Air traffic flow management integrating separation management and ground holding: An efficiency-equity bi-objective perspective[J]. *Transportation Research Part B: Methodological*, 2022, 155: 394-423.
- [24] HAMDAN S, CHEAITOU A, JOUINI O, et al. Central authority-controlled air traffic flow management: An optimization approach[J]. *Transportation Science*, 2022, 56(2): 299-321.
- [25] REY D, RAPINE C, DIXIT V V, et al. Equity-oriented aircraft collision avoidance model[J]. *IEEE Transactions on Intelligent Transportation Systems*, 2014, 16(1): 172-183.
- [26] ZHANG H H, HU M H. Multi-runway collaborative scheduling optimization of aircraft landing[J]. *Journal of Traffic and Transportation Engineering*, 2009, 9(3): 86-91.
- [27] GUTIERREZ-NOLASCO S, SHETH K. Analysis of factors for incorporating users preferences in air traffic management: A user's perspective[C]//*Proceedings of the 10th AIAA Aviation Technology, Integration, and Operations (ATIO) Conference*. Fort Worth, USA: [s.n.], 2010: 9063.
- [28] WANG G, JIA H, FENG T, et al. An acceptability-based multi-objective traffic flow adjustment method for environmental sustainability and equity[J]. *Journal of Cleaner Production*, 2023, 418: 138077.
- [29] RUIZ S, PIERA M A. Relational time-space data structure to enable strategic de-confliction with a global scope in the presence of a large number of 4D trajectories[J]. *Journal of Aerospace Operations*, 2013, 2(1/2): 53-78.
- [30] RUIZ S, PIERA M, ZUNIGA C. Relational time-space data structure to speed up conflict detection under heavy traffic conditions[J]. *Journal of Aerospace Operations*, 2013, 2(1/2): 53-78.
- [31] METROPOLIS N, ROSENBLUTH A W, ROSENBLUTH M N, et al. Equation of state calculations by fast computing machines[J]. *The Journal of Chemical Physics*, 1953, 21(6): 1087-1092.
- [32] COOK A, TANNER G. *European airline delay cost reference values*[R]. Brussels, Belgium: Eurocontrol, 2015.

Acknowledgements This work was supported by the National Key R&D Program of China (No.2022YFB4300905), the National Natural Science Foundation of China (No. 61903187), the Natural Science Foundation of Jiangsu Province (No.BK20190414).

Authors Mr. ZHOU Yi is currently a Ph.D. student at College of Civil Aviation, Nanjing University of Aeronautics and Astronautics (NUAA). His research interests include air traffic flow management and planning.

Prof. HU Minghua is currently a professor and doctoral supervisor at the College of Civil Aviation, NUAA. He is the director of National Key Laboratory of Air Traffic Flow Management of China and executive deputy director of the

State Key Laboratory of Air Traffic Management System in NUAA. His research interests include air traffic flow management and airspace management.

Author contributions Mr. ZHOU Yi proposed the architecture for the MHMOA algorithm and wrote the manuscript. Prof. HU Minghua summarized the existing studies and designed the optimization model. Dr. YANG Lei

contributed to the discussion of the experiments and the result analyses. Dr. ZHANG Ying contributed to the discussion and background of the study. All authors commented on the manuscript draft and approved the submission.

Competing interests The authors declare no competing interests.

(Production Editor: ZHANG Bei)

基于多目标混合启发式算法的协同无冲突4D航迹规划

周逸^{1,2}, 胡明华^{1,2}, 杨磊^{1,2}, 张颖^{2,3}

(1. 南京航空航天大学民航学院, 南京 211106, 中国; 2. 空中交通管理系统全国重点实验室, 南京 211106, 中国; 3. 南京航空航天大学通用航空与飞行学院, 南京 211106, 中国)

摘要:为促进基于航迹运行的框架下未来空中交通管理系统的协同决策,本文提出了一种协同无冲突4D航迹规划方法。首先以提高航班效率和航空公司间的公平性为目标,以无冲突为约束构建了一个多目标整数线性优化模型。其次,提出了一种基于基尼系数的指标以量化航空公司间的成本分配公平性。为了提高问题求解效率,采用了基于网格的探测方法以加速冲突检测,并设计了一种多目标混合启发式算法(Multi-objective hybrid-meta-heuristic optimization algorithm, MHMOA),通过结合模拟退火(Simulated annealing, SA)和爬山局部搜索算法来近似最优的非支配解。最后,利用实际航班计划和航路网络数据比较和分析了MHMOA、SA和两种常规多目标优化算法的优化结果。结果表明,MHMOA所获得的非支配解的质量更高、延误更低且航空公司间公平性更优,在3个多目标优化性能指标方面表现优异,可为空中交通管理员提供更详细的决策支持。

关键词:空中交通管理;航迹规划;混合启发式算法;4D航迹;多目标优化